Available online at www.sciencedirect.com
SCIENCE DIRECT®
Vibrational Spectroscopy 34 (2004) 37–45
VIBRATIONAL SPECTROSCOPY
www.elsevier.com/locate/vibspec

Infrared spectroscopy and spectroscopic imaging of *n*-propyl trichlorosilane monolayer films self-assembled on glass substrates

Douglas L. Elmore[a,*], D. Bruce Chase[b], Yujuan Liu[c], John F. Rabolt[c]

[a]*Cargill Scientific Resources Center, Cordova, TN 38016, USA*
[b]*Central Research and Development, DuPont Experimental Station, Wilmington, DE 19880-0328, USA*
[c]*Department of Materials Science and Engineering, University of Delaware, Newark, DE 19716-3106, USA*

Abstract

Monolayer films of *n*-propyl trichlorosilane (PTS) self-assembled on glass substrates were investigated using Fourier transform infrared spectroscopy (FTIR) and planar array infrared spectroscopic imaging (PA-IR spectroscopic imaging) as a function of three different solvents (hexane, benzene and toluene). The alkyl chain of a PTS monolayer has only two conformational isomers, g*auche* and *trans*. In this study, we show that the two isomers give rise to significantly different transmission IR spectra in the aliphatic stretching region for both 0° and 15° angles of incidence. The *gauche* spectrum is dominated by $\nu(CH_3)$ contributions, while the *trans* spectrum has large $\nu(CH_2)$ contributions. These observations can be explained in terms of the orientation of the $\nu_a(CH_3)$ and $\nu_s(CH_3)$ and the $\nu_a(CH_2)$ and $\nu_s(CH_2)$ transition dipole moments. The distinct difference between a g*auche* and *trans* spectrum can serve as a probe for conformational order in PTS monolayers. In general, relatively low total integrated absorbance values were associated with disordered films, while relatively high values were associated with ordered films. A plot of the 2925 cm^{-1}/2960 cm^{-1} peak intensity ratios versus total integrated absorbance suggests the existence of an ordered and disordered phase above and below ∼58% surface coverage, respectively. Under the conditions of this study, the most ordered PTS monolayers films were prepared with hexane while less ordered monolayers were produced using benzene. Only disordered films were produced with toluene. When compared with a previous study (Langmuir (in press)), the relative ability of these three solvents to produce an ordered PTS or *n*-octadecyl trichlorosilane (OTS) monolayer film follow a similar trend. We also report the first broad band infrared line images of a short chain monolayer film, which were obtained with a PA-IR spectrograph. The line images of PTS monolayers revealed both relatively homogeneous and heterogeneous regions in terms of conformational order.

Keywords: *n*-Propyl trichlorosilane; *n*-Octadecyl trichlorosilane; Infrared spectroscopy; Infrared imaging; Planar array infrared spectrograph; Self-assembled monolayer

1. Introduction

The self-assembled architecture of alkyl trichlorosilane monolayer films has received and continues to receive considerable attention in both fundamental and applied research [2,3]. Well ordered monolayer films, prepared using long chain alkyl trichlorosilanes, such as octadecyl trichlorosilane (OTS), have been studied extensively in the areas of semiconductor and sensor coatings [4–6], nanolithography [7,8] and biomembrane model systems [9]. Conversely, short chain alkyl trichlorosilane monolayers have received little attention, in part because well ordered films are not as easily prepared as their long chain counter parts and the shorter chain monolayers find fewer applications [10–12]. However, a better understanding of both short and long chain alkyl monolayers is necessary to more fully characterize the properties of self-assembled alkyl trichorosilane monolayers in general. For this reason we report an infrared spectroscopic and imaging study of *n*-propyl trichlorosilane (PTS) monolayer films self-assembled on glass substrates. PTS was chosen because its alkyl chain, like butane, only exists in one of two conformational isomers, *gauche* or *trans*. In this work it it is shown that these two isomers produce significantly different infrared spectra when measured at 0° or 15° degree angles of incidence. These spectral differences are exploited to probe conformational order as a function of solvent used to prepare the monolayer film.

Conventional Fourier transform infrared spectroscopy (FTIR) has been used extensively to probe the conformational order and molecular orientation of monolayer films assembled on both metallic and dielectric substrates [13–15]. The ability of FTIR spectroscopic imaging to provide spatially resolved spectra [16–21] has recently gained

* Corresponding author. Tel.: +1-901-775-5945; fax: +1-901-937-4531.
E-mail address: doug_elmore@cargill.com (D.L. Elmore).

0924-2031/$ – see front matter © 2003 Elsevier B.V. All rights reserved.
doi:10.1016/j.vibspec.2003.09.007

considerable attention, and the extension of this technique to monolayer films would be extremely interesting. Unfortunately, to date, FTIR imaging spectrometers have not provided the necessary sensitivity for monolayer measurements [22,23]. Recently, Elmore et al. [24] described the design and performance of a broadband planar array infrared (PA-IR) spectrograph that can be used to obtain spatially resolved spectra with high sensitivity, and reported the first spatially resolved infrared spectra (line images) of a self-assembled monolayer (*n*-octadecyl trichlorosilane (OTS) on glass). The same PA-IR spectrograph was used in this study, and we now report the first spatially resolved infrared spectra (line images) of a short chain self-assembled monolayer (PTS on glass).

2. Experimental

2.1. PTS monolayer films self-assembled on glass

n-Propyl trichlorosilane (PTS) was obtained from Aldrich at >98% purity. Toluene (HPLC grade), hexane (HPLC grade) and benzene (ACS grade) were obtained from Fisher Scientific. The solvents used in the cleaning process were 30% H_2O_2, 37.8% HCl and 29.8% NH_4OH (all certified ACS grade, Fisher Scientific). All chemicals listed above were used without further purification. Ultrapure water (resistivity 18.2 MΩ cm, Millipore Ultrapure water system, Millipore Inc.) was used throughout the cleaning procedure.

BK-7 glass microscope slides (7.5 cm:2.5 cm), Fisherbrand, Fisher Scientific) were cleaned according to a standard procedure [25]. The slides (five slides per cleaning batch) were immersed in a NH_4OH:H_2O_2:H_2O (1:1:5) solution at 65 °C for 15 min, rinsed in water for 10 min, followed by immersion in a HCl:H_2O_2:H_2O (1:1:5) solution at 65 °C for 15 min, rinsed in water for 10 min and finally dried in a flow of warm, clean nitrogen gas. One of the cleaned slides was immediately stored under nitrogen and used for collecting the reference IR spectra.

PTS solutions were prepared at 1 mM concentration under a nitrogen atmosphere and used immediately. The cleaned slides were immersed into vials containing the freshly prepared solutions and sealed with parafilm under nitrogen. The coated slides were then taken out after an hour and rinsed using the respective solvents and dried using warm nitrogen.

2.2. Planar array infrared spectroscopic imaging

The optical configuration for the PA-IR spectrograph used in this study is the same as previously described [1], with the exception that the sample was placed in front of the adjustable entrance slit. The instrument employed a glow bar light source, an f/2.5 Czerny-Turner type grating monochromator and an InSb focal plane array infrared camera.

The spectrograph was constructed on a Newport (NRC) optical table without an operational vibration–isolation system. The globar is ∼3 cm high with ∼10 mm diameter wide and is driven by a regulated power supply. The adjustable entrance slit was opened to width of ∼0.3 mm. The integration time was 1.5 ms per frame. The ruled grating has 300 grooves/mm (SPEX, Edison, NJ) and a blaze wavelength of 4.0 μm. The 320 × 256 focal plane array, with 30 μm × 30 μm pixels, is housed in the dewar of a Merlin™ InSb Laboratory Infrared Camera (Indigo Systems, Santa Barbara, CA). A resolution element, defined by the pixel size and the spectral dispersion, was approximately 5 cm^{-1}, and the observed spectral resolution at ∼2920 cm^{-1} was about 6 cm^{-1} as determined by comparison of PA-IR and FTIR spectra.

A two-point non-uniformity correction of the FPA response was performed at the beginning of the study with a 1.5 ms integration time using ∼75% of the camera's dynamic range. One-point non-uniformity corrections were performed prior to data acquisition. The method for performing both corrections has previously been described [24].

Raw spectral data files were collected and saved as 320 × 256 images (TIF) using Image-Pro Plus software (Media Cybernetics, Silver Spring, MD) and a personal computer with a 650 MHz processor and 256 MB of RAM. The frame rate was 60 frames/s.

In the PA-IR spectrograph the slit image is dispersed across the FPA, and the resulting image is referred to as a spectral image. Spectral absorbances were observed for PTS in the ∼3200–2600 cm^{-1} region. The spectral image is about 120 pixel rows high and about 200 pixels wide. All infrared line images presented in this paper were obtained by averaging 18,000 frames. Ratioed spectra were calculated using Image-Pro Plus and Excel (Microsoft, Redmond, WA) as previously described [24]. The spectra were plotted using GRAMS/32 (Galactic Industries, Salem, NH).

In a PA-IR spectral image, absorbances shift in an arc like pattern as individual pixel rows are observed from the top to the bottom of the line image [1,24]. This effect is commonly referred to as "slit curvature" and is dependent on the f-number of the monochromator. To eliminate the slit curvature, the pixel numbers for each individual row are normalized against the first pixel row in the line image (with a sample placed in the sample holder). In other words, the intensity versus pixel number plot for each pixel row is calibrated against the intensity versus pixel number plot of the first row in the line image and the observed peaks in each pixel row are forced to line up at the same pixel column number. This is equivalent to a row-dependent frequency shift that corrects for the optical slit curvature.

PA-IR spectra for the PTS monolayer film prepared with hexane were collected with a spatial resolution of 200 μm. PA-IR spectra for the film prepared with toluene were also collected with a spatial resolution of 200 μm; however in this case, every four spatially resolved spectra were averaged to increase the signal-to-noise ratio (SNR), resulting in a final spatial resolution of 800 μm. The rows were averaged prior to the correction for slit curvature

to reduce the data reduction time. Signal averaging just four rows prior to the correction for slit curvature produces an error in frequency of <0.2 cm^{-1}. Frequencies in the PA-IR spectra were calibrated using a method previously described [24].

2.3. Fourier transform infrared spectroscopy

FTIR spectra were measured at 4 cm^{-1} resolution using a Nexus 870 FTIR spectrometer (Thermo Nicolet, Madison, Wisconsin) with unpolarized light and a DTGS detector. Each spectrum was apodized with a triangular function and one level of zero filling. The angles of incidence are noted as each spectrum is presented in the Results and Discussion section. The first set of spectra, presented in Fig. 1, were obtained by signal averaging 18,000 scans. Subsequent spectra were obtained by signal averaging either 1000 or 2000 scans to obtain an acceptable SNR. All PTS monolayer single beam spectra were ratioed against clean glass slides. The PTS bulk single beam and the corresponding background spectrum were obtaining using KBr disks. The peak frequencies were determined from the band maxima using the GRAMS/32 program.

A simple two point baseline correction was applied to all of the FTIR and PA-IR spectra except for the multiple angle (0°, 15° and 75°) spectra. Each of the multiple angle spectra were baseline corrected with a quadratic function to compensate for a curved baseline, which appeared most dramatically in the 75° spectrum. The quadratic correction was obtained by fitting on the baseline above 3000 cm^{-1} and below 2825 cm^{-1}. In order to further increase the SNR, the spatially resolved PA-IR spectra for the monolayer prepared with toluene were smoothed with a Savitzky-Golay algorithm in which 25 points were fit to a second order polynomial. No other spectra in this article have been smoothed including the spatially resolved PA-IR spectra for the monolayer prepared with hexane. Peak frequencies were determined with second derivatives calculated with a Savitzky-Golay algorithm in which five points were fit to a second order polynomial. The 2925 cm^{-1}/2960 cm^{-1} peak height ratios were determined using the absorbance maxima near 2925 cm^{-1} and 2960 cm^{-1}.

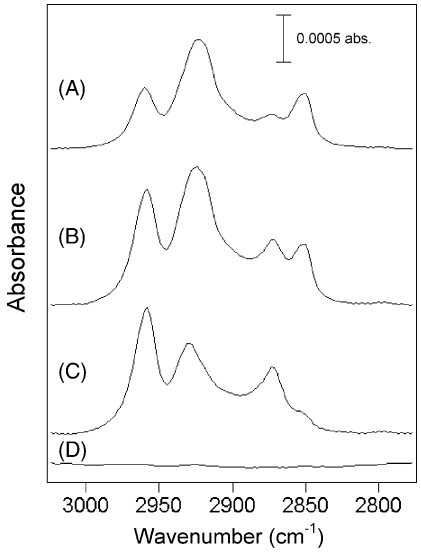

Fig. 1. FTIR spectra of PTS monolayers self-assembled on glass using (A) hexane, (B) benzene, (C) toluene as a solvent; and (D) a 100% line produced by ratioing the single beam spectra of two clean glass slides.

3. Results and discussion

3.1. Fourier transform infrared spectroscopy

A series of self-assembled PTS monolayer films were prepared on glass substrates using hexane, benzene and toluene as solvents. FTIR spectra of these films were collected at normal incidence and three examples are presented in Fig. 1A–C, respectively. A 100% line for the C–H stretching region was also produced by ratioing the single beam spectra of two clean glass slides and is presented in Fig. 1D. The line demonstrates that no detectable changes in alkylated contamination are observed from one slide to the next.

In Fig. 1A–C, three different shaped spectra are observed in the aliphatic stretching region depending on the solvent used. The spectrum in Fig. 1B (benzene) may be considered approximately as a linear combination of the spectra in Fig. 1A and C (hexane and toluene). In all three spectra, the $\nu_a(CH_3)$ band is observed at ~2960 cm^{-1}, while the $\nu_s(CH_3)$ band, which is split by Fermi resonance interaction with $\delta(CH_3)$ [26–28], is observed at ~2873 and ~2930 cm^{-1} (the latter band appearing most prominently in Fig. 1C). In Fig. 1A, the $\nu_a(CH_2)$ and $\nu_s(CH_2)$ bands, which are sensitive to conformational order in the alkyl chains [27], are observed at ~2917.0 and 2849.4 cm^{-1}, respectively. These frequency values are consistent with an ordered phase [2] and suggest that the alkyl chains of the monolayer prepared with hexane are present in a mostly all-*trans* conformation. In contrast, the frequency of $\nu_s(CH_2)$ band for the monolayer prepared with toluene (Fig. 1C) is observed at 2952.0 cm^{-1} (for this spectrum, the frequency of the relatively small $\nu_a(CH_2)$ band could not be accurately determined in the presence of the relatively large $\nu_s(CH_3)$ Fermi resonance band). The observed 2 cm^{-1} difference between the $\nu_s(CH_2)$ bands for the two different PTS films in Fig. 1A and C is consistent with the calculated 2 cm^{-1} difference between *trans* and *gauche* conformers for butane (a convenient model for the alkyl chain in PTS) reported by Snyder [29]. The $\nu_s(CH_2)$ band frequency therefore suggests that the monolayer prepared with toluene (Fig. 1C) exists in a disordered phase in which the alkyl chains are present in a mostly *gauche* conformation. The frequencies of the $\nu_a(CH_2)$ and $\nu_s(CH_2)$ bands for the monolayer prepared with benzene (Fig. 1C) are observed at 2918.5 cm^{-1} and 2949.9 cm^{-1}, respectively. Since the observed frequency of

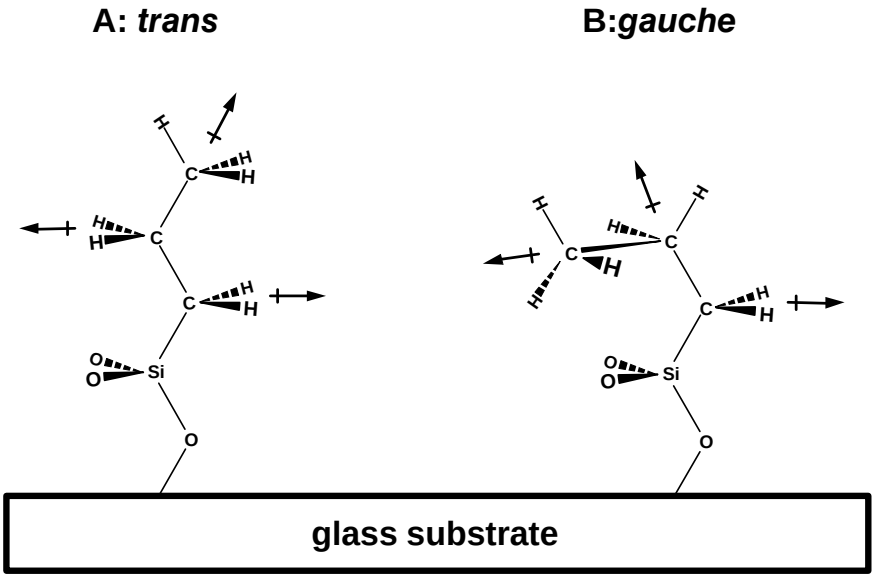

Fig. 2. The alkyl chain of a PTS monolayer film exists as either (A) a *trans* or (B) a *gauche* conformational isomer.

the $\nu_a(CH_2)$ band is probably skewed to a larger value by the presence of the $\nu_s(CH_3)$ Fermi resonance band, this band will not be considered further. The $\nu_s(CH_2)$ band frequency suggests that the monolayer prepared with benzene possesses less conformational order than film prepared with hexane, but more conformational order than the film prepared with toluene.

The spectrum of the film prepared with hexane features relatively strong CH_2 contributions, while the spectrum of the film prepared with toluene features relatively strong CH_3 contributions. These observations can be explained by considering the different possible conformational states of alkyl chains in the monolayer and the orientation of the transition dipole moments relative to the electric field of the incident beam. Like butane, the alkyl chain in a PTS monolayer exists as one of two conformational isomers, i.e., *gauche* or *trans*. A model representation of both conformers is presented in Fig. 2.

The transition dipole moments for the $\nu_a(CH_2)$ and $\nu_s(CH_2)$ vibrations in the *trans* conformer are aligned perpendicular to the chain axis, while the $\nu_s(CH_3)$ vibration has a transition dipole moment that is parallel to the C–CH_3 bond. The $\nu_a(CH_3)$ band is composed of both in-plane (ip) and out-of-plane (op) modes. The transition dipole moment for the $\nu_a(CH_3$, ip) band is perpendicular to the C–CH_3 bond and parallel to the C–C plane of an all-*trans* alkyl chain. The transition dipole moment for the $\nu_a(CH_3$, op) band is perpendicular to both the $\nu_a(CH_3$, ip) and the $\nu_s(CH_3)$ transition dipole moments. The approximate orientations of the transition dipole moments for the $\nu_s(CH_2)$ and $\nu_s(CH_3)$ vibrations are identified with crossed arrows in Fig. 2A. For simplicity only the $\nu_s(CH_2)$ and $\nu_s(CH_3)$ vibrations are considered in the orientation argument that follows; however, it should be noted that similar arguments apply to the $\nu_a(CH_2)$ and $\nu_a(CH_3)$ vibrations.

In this model, we assume that the *trans* chain axis is oriented approximately normal to the substrate surface, that is to say the tilt angle is $\sim 0^\circ$. The assumption seems reasonable since previous studies have reported average tilt angles between 5° and 15° for self-assembled monolayers derived from n-alkyl trichlorosilane [30,31]. In the case of small tilt angles, the $\nu_s(CH_2)$ vibrations have a very large component in the plane of the substrate, while the $\nu_s(CH_3)$ vibration has a significant component perpendicular to the substrate. This results in the observation of a relatively large ratio of the $\nu_s(CH_2)$ to the $\nu_s(CH_3)$ absorbance values for PTS films with a large population of *trans* conformers (well ordered films).

The situation is nearly reversed for the *gauche* conformers, i.e., the $\nu_s(CH_3)$ transition dipole moment has a very large component aligned parallel to the substrate, while the $\nu_s(CH_2)$ vibration has a more significant component perpendicular to the substrate (see the crossed arrows in Fig. 2B). This results in the observation of a relatively large ratio of $\nu_s(CH_3)$ to $\nu_s(CH_2)$ absorbance values for PTS films with a large population of *gauche* conformers (disordered films). It should be noted that some portions of the film may exist in which the chain axis is present in a *trans* conformation and is bent toward the substrate approaching a tilt angle of $\sim 90^\circ$. The resulting spectral contributions would not be easily distinguished from the *gauche* contributions in the 3000 to 2800 cm^{-1} region. However, any *trans* conformers with very large tilt angles would surely be associated with a disordered region of the film, and therefore conclusions drawn from the spectra concerning relative order should not be compromised by this contribution.

FTIR spectra of another PTS monolayer prepared with hexane are presented in Fig. 3A–C. These spectra were collected at 0°, 15° and 75° angles of incidence. In addition, an FTIR spectrum of unreacted, bulk PTS is presented in

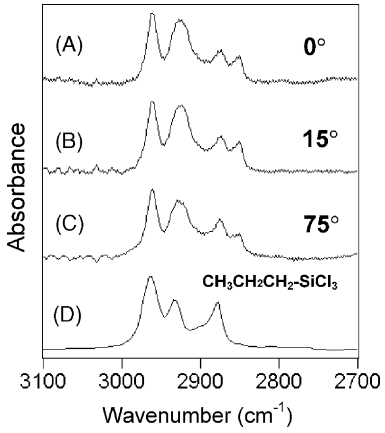

Fig. 3. FTIR transmission spectra of a PTS monolayer on a glass slide collected at (A) 0°, (B) 15° and (C) 75° angles of incidence; and (D) an FTIR spectrum of unreacted, bulk PTS. The maximum absorbance value for each spectrum in this figure has been normalized to the same value.

Fig. 3D. Comparison of the 0° and 15° spectra reveals little difference, while the 75° spectrum features a larger CH_3 component than the 0° spectrum. The observations are consistent with the *gauche* versus *trans* orientation argument presented earlier. The fact that the 0° and 15° spectra are quite similar is pertinent to the PA-IR spectroscopic imaging discussion.

With no prior knowledge of the PTS structure, one might conclude from the spectra in Fig. 3A and D that the PTS monolayer contains both CH_3 and CH_2 groups, while the unreacted, bulk PTS only contains CH_3 groups. This of course is not the case. In actuality, the strong inductive effect of the $SiCl_3$ group on the $\nu(CH_2)$ shifts the vibrations to higher frequencies in Fig. 3D resulting in a spectrum in which the $\nu(CH_3)$ and $\nu(CH_2)$ bands are unresolved [32]. In the case of a self-assembled PTS monolayer, all of the Si–Cl bonds have been converted to either a Si–O–Si or a Si–OH bond [10]. However, any remaining hydroxyl groups on the PTS Si atom may have an effect on the frequency and intensity of the $\nu(CH_2)$ bands. While a stronger electronic effect is expected from a Si–OH bond than a Si–O–Si bond, this effect should be weaker than the strong electron withdrawing effect produced by a $SiCl_3$ group. If an inductive effect on the $\nu(CH_2)$ does exist, the resulting monolayer spectrum may appear to contain more $\nu(CH_3)$ contributions. However, it is unlikely that such an effect would significantly impact any qualitative conclusions drawn from the spectra since a monolayer with mostly *trans* conformers is clearly distinguished from a monolayer with mostly non-*trans* conformers (see Fig. 1A and C).

It should also be noted that some –O–Si–O– linkages may exist between neighboring PTS molecules whose silicon atoms are not chemically bound to the substrate [10]. The additional freedom would allow the *gauche* $\nu_s(CH_2)$ transition dipole moments to orient in positions that further decrease the component parallel to the substrate, resulting in even larger $\nu(CH_3)/\nu(CH_2)$ absorbance ratios for disordered films than suggested by the simple model depicted in Fig. 2. And finally, the model in Fig. 2 does not account for possible rotation of the alkyl group around the C–Si bond to the next energy minima (staggered). Rotation around the C–Si bond to the next staggered position would also allow the *gauche* $\nu_s(CH_2)$ transition dipole moments to orient in positions that further reduce the component parallel to the substrate.

Table 1
Total integrated absorbance for the CH_2/CH_3 stretching region and corresponding 2925/2960 cm^{-1} peak height ratios

Solvent	Total integrated absorbance[a]			Peak height ratios[b]		
	Low	High	Average	Low	High	Average
Hexane	0.020	0.130	0.069	0.78	1.81	1.22
Benzene	0.017	0.102	0.048	0.56	1.19	0.77
Toluene	0.021	0.079	0.046	0.61	0.82	0.70

[a] Total integrated absorbance values were determined between 2985 and 2825 cm^{-1}.

[b] Peak height ratios were determined from the peak maxima near 2925 and 2960 cm^{-1}.

As mentioned before, it seems reasonable to consider all of the spectra observed in this study as some linear combination of the mostly *trans* (hexane) and mostly *gauche* (toluene) spectra presented in Fig. 1A and C. It then follows that the 2925 cm^{-1}/2960 cm^{-1} peak height ratio serves as a convenient parameter for monitoring relative conformational order in the alkyl chains. The range and average for both the 2925 cm^{-1}/2960 cm^{-1} band ratios and the total integrated absorbance values are therefore presented in Table 1 for the entire series of PTS monolayer films.

Based on the average band ratio, hexane produced the most ordered PTS monolayer films (1.22), which also had the highest average total integrated absorbance (0.069). However, under the same apparent conditions, several disordered films (0.78 and 0.79) were also obtained using hexane, which had relatively low total integrated absorbance values (0.0201 and 0.0204). When compared with toluene, benzene produced films with only slightly larger average ratios (0.77 versus 0.70) and average absorbance values (0.048 versus 0.046). One ordered film was produced by benzene that featured a relatively high ratio (1.19). No significantly ordered films were prepared with toluene (ratios all <0.83). The lack of reproducibility in the films prepared with hexane and benzene reflects the difficulty in producing an ordered PTS monolayer due to the short alkyl chain length. These film variations can be exploited to reveal a relationship between order and surface density as follows.

A plot of 2925 cm^{-1}/2960 cm^{-1} peak height ratio versus total integrated absorbance was constructed for the entire monolayer film series and is presented in Fig. 4. In this plot, two distinct regions are observed and are emphasized by dashed lines added to the figure. The first region is located between ~0.017 and 0.075 total absorbance and contains relatively low 2925 cm^{-1}/2960 cm^{-1} peak height ratios ranging from ~0.56 to 0.72. The second region is located

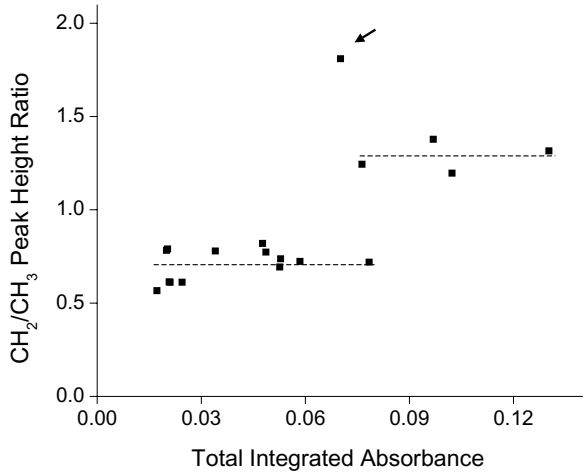

Fig. 4. A plot of 2925 cm^{-1}/2960 cm^{-1} peak height ratio vs. total integrated absorbance obtained from the spatially averaged monolayer spectra.

between ~0.075 and 0.13 total absorbance and contains relatively high ratios ranging from ~1.19 to 1.31. We therefore conclude that the first region corresponds to a disordered phase; the second region corresponds to an ordered phase, and the two phases are separated by a narrow transition region. While the relationship between surface density and total integrated absorbance is clearly complicated by orientation effects, the lowest and highest absorbance values vary by approximately eight fold. It therefore seems reasonable to qualitatively attribute the largest absorbance values to relatively large surface densities and the lowest absorbance values to relatively low surface densities. If we assume the largest total integrated absorbance value corresponds to ~100% surface coverage, we can roughly estimate that the phase transition region occurs near $0.075/0.13 = 58\%$ surface coverage.

The measurement located at (0.070, 1.81), which is identified by a solid arrow (Fig. 4), corresponds to the most ordered film prepared in the study and appears to be an outlier. Two possible explanations are proposed. (1) Since this is the most ordered film observed in the study, the film may be described by a third phase (more ordered) in which the tilt angle of the alkyl chain has shifted to a more out-of-plane orientation relative to the substrate. A very small change in surface coverage could give rise to a significant change in tilt angle, resulting in a slightly increased $\nu(CH_2)$ contribution and a significantly decreased $\nu(CH_3)$ contribution. A large enough decrease in the $\nu(CH_3)$ component would actually lower the total integrated absorbance value. (2) PTS monolayer islands may have formed on the glass substrate in such a way that surface density is high in the island and low between islands. Islands are known to form in long chain alkyl trichlorosilane monolayers on glass substrates [7,33]. In the future, morphologically sensitive techniques such as AFM and SEM will be included to investigate these possibilities.

Finally, it is noted that a solvent dependent study of OTS monolayer films on glass substrates using hexane, benzene and toluene as solvents was recently described by Elmore et al. [1]. The relative ability of these three solvents to produce both ordered PTS and OTS monolayer films follow a similar trend, although it is more difficult to obtain an ordered PTS film under the same conditions. It is clear that the variation in conformational disorder in PTS monolayers, as with OTS [1], is not controlled solely by choice of solvent, but involves other yet undefined experimental parameters.

3.2. Planar array infrared spectroscopic imaging

Spatially resolved information about the PTS monolayer films was obtained using a PA-IR spectrograph. An example of 40 spatially resolved PA-IR spectra (IR line image) is presented in Fig. 5A for a film prepared using hexane. The line image has a spatial resolution of 200 μm and corresponds to a 300 μm width (defined by the spectrograph's slit width) and an 8.0 mm length of the monolayer. The 300 μm × 8.0 mm field of view is somewhat arbitrary and is located near the center of the slide. The slide is 2.5 cm wide and 7.5 cm long, and the edge of the line image does not correspond to the edge of the slide. The spectroscopic measurements were originally attempted at normal incidence, but unfortunately large interference fringes were observed. It was then noted that the interference fringes were reduced to acceptable level when a 15° angle of incidence was used. Since it was found that either 0° or 15° spectra could be used to monitor the *trans* to *gauche* ratio in PTS films (see Fig. 3A and B), the higher quality 15° PA-IR spectra were collected.

For the spectra in Fig. 5A, the total integrated absorbance values ranged from 0.0924 to 0.1121,[1] while the 2925 cm^{-1}/2960 cm^{-1} peak height ratios ranged from 1.09 to 1.15. All absorbance and ratio values in these ranges are consistent with an ordered film (see Fig. 4). The region between ~4.0 and 8.0 mm appears to be relatively homogeneous in terms of both conformational order and surface density, while the region between ~4.0 and 0.0 mm shows some variation. Specifically, the film gradually loses some chain order and surface density from ~4.0 to 0.0 mm in a smooth continuous manner. When we consider that the PTS molecule is no more than ~1 nm wide, it appears that the order changes at a fairly slow rate in the spatial domain. The relatively homogeneous region of the monolayer certainly appears to have some degree of long range order. It may be possible to attribute the smooth variation in chain order in the more heterogeneous region of this film to a loss of some conformational order while maintaining some long range order.

Similar degrees of homogeneity were observed qualitatively in most regions of the films produced with any of the

[1] An increase of ~4% in the total integrated absorbance for 15° compared to 0° angle of incidence measurements is expected due to the slightly increased length of the slide sampled by the IR beam.

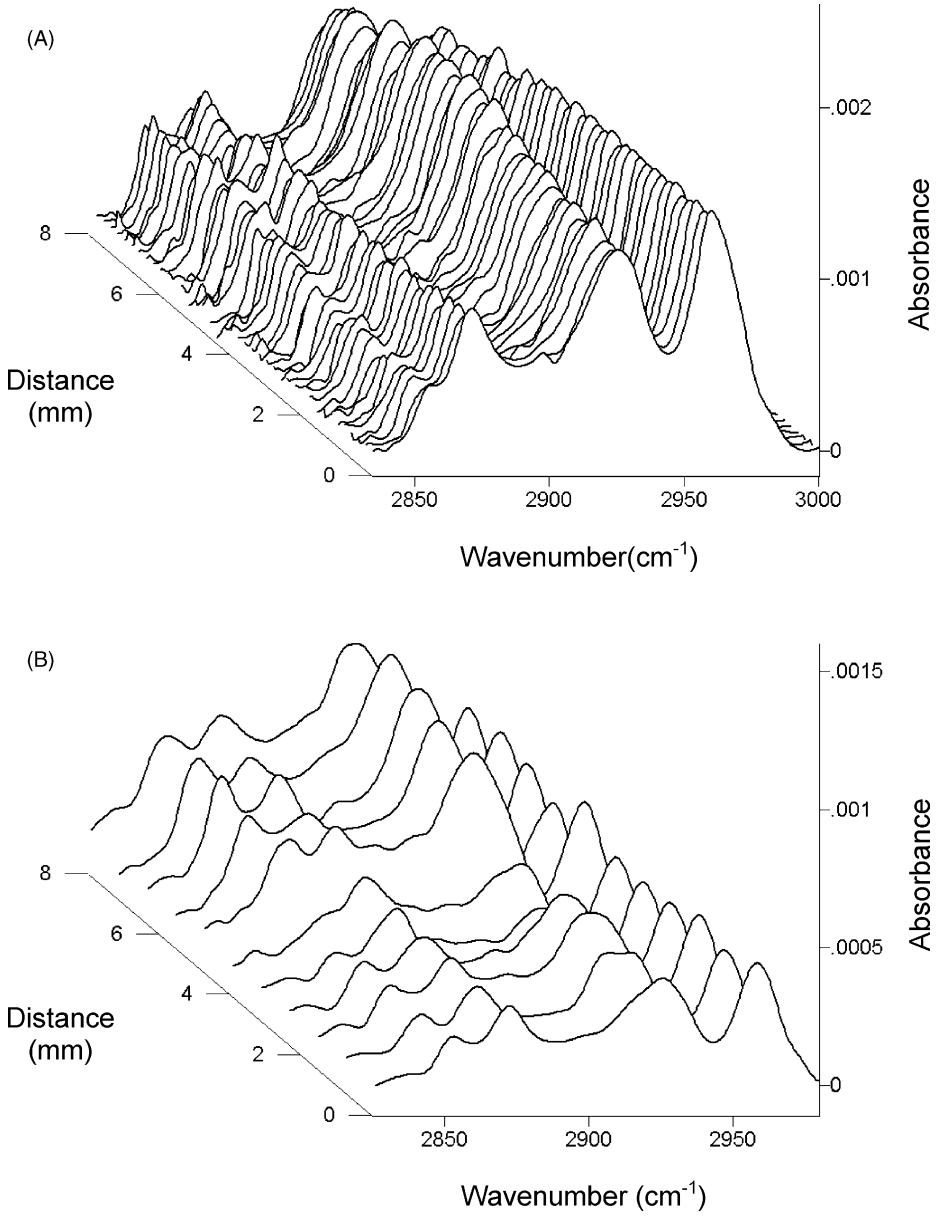

Fig. 5. Examples of spatial resolved PA-IR spectra (line image) for a PTS monolayer self-assembled with (A) hexane and (B) toluene.

three solvents. However, some spatially dependent variations in chain order were also observed for films prepared with any of the three solvents. The largest variations were observed for films prepared with benzene and toluene. As an example, 20 spatially resolved PA-IR spectra (IR line image) are presented in Fig. 5B for a film prepared with toluene. This line image has a spatial resolution of 800 μm and also corresponds to a 300 μm × 8.0 mm field of view. Again, the field of view is somewhat arbitrary and is located near the center of the slide. In contrast to Fig. 5A, the spatially resolved spectra of this image reveal a heterogeneous region in terms of conformational order and surface density.

Plots of the 2925 cm^{-1}/2960 cm^{-1} peak height ratio versus total integrated absorbance and distance were constructed based on the spectra in Fig. 5B. The two plots are presented in Fig. 6A and B, respectively. In Fig. 6A, the total integrated absorbance values ranged from 0.02542 to 0.05207, while the 2925 cm^{-1}/2960 cm^{-1} peak height ratios ranged from 0.75 to 1.74. The smoothing algorithm skews the absolute peak height ratio toward higher values, and thus can only be considered relatively within the set. However, when the spatially resolved spectra in Fig. 5B are individually inspected it is clear that there are regions in the film that range from very disordered to very well ordered. It is particularly interesting to observe some ordered regions in a film with such a low average total integrated absorbance (0.0376) and thus low surface density.

Fig. 6B reveals a disordered region of the monolayer located between ∼0.0 and 4.0 mm and an ordered region located between ∼6.0 and 8.0 mm. The existence of both

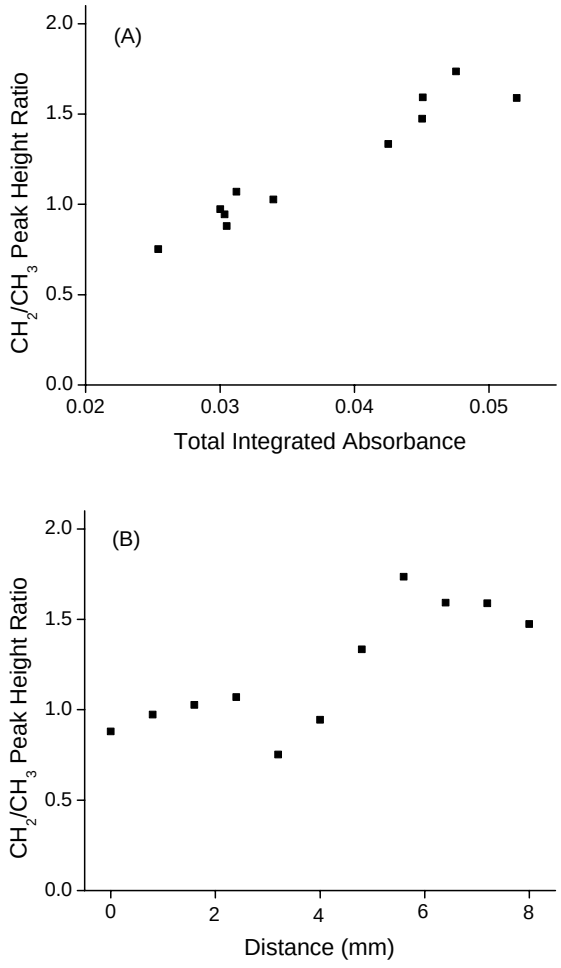

Fig. 6. A plot of 2925 cm^{-1}/2960 cm^{-1} peak height ratio vs. (A) total integrated absorbance and (B) distance in millimeters obtained from the spatial resolved spectra for a PTS monolayer film prepared with toluene.

ordered and disordered regions in the same film could possibly be explained by the existence of ordered islands of PTS monolayers on the glass substrate. As mentioned earlier, morphologically sensitive methods such as AFM and SEM will be included in future studies. Future PA-IR studies will include beam condensing optics for obtaining diffraction limit spatial resolution, i.e., ~5 μm in the aliphatic stretching region.

4. Conclusions

Gauche and *trans* conformers in self-assembled PTS monolayers on glass substrates produce significantly different spectra in the aliphatic stretching region when transmission measurements are made at 0° or 15° angles of incidence. This observation can be explained in terms of the relative orientation of the $\nu(CH_2)$ and $\nu(CH_3)$ transmission dipole moments in the infrared electric field. Disordered films, which contain mostly *gauche* conformers, are dominated by $\nu(CH_3)$ components, while conversely, highly ordered films, which contain mostly *trans* conformers, have significant $\nu(CH_2)$ components. These spectral differences form the basis for monitoring conformational order in PTS monolayer films. In general, relatively low total integrated absorbance values are associated with disordered films, while relatively high values are associated with ordered films. A plot of 2925 cm^{-1}/2960 cm^{-1} peak height versus total integrated absorbance suggests that conformational order increases as a function of surface density and reveals the existence of an ordered and disordered phase above and below ~58% surface coverage, respectively.

Under the conditions of this study and on the average, hexane produces the most ordered PTS monolayers films, followed by benzene. No significantly ordered films were prepared using toluene. When compared with a previous study [1], the relative ability of these three solvents to produce an ordered PTS or OTS monolayer film follow a similar trend. However, it is more difficult to obtain an ordered PTS film under the same conditions. It is clear that the variation in conformational disorder in PTS monolayers, as with OTS [1], is not controlled solely by choice of solvent, but involves other yet unidentified experimental parameters.

A PA-IR spectrograph can be used to obtain broad band infrared line images of short chain monolayer films with reasonable SNR for probing spatial variations in conformational order. The line images of PTS monolayers revealed both relatively homogeneous and heterogeneous regions in terms of conformational order. Relative order increases in the spatial domain as surface density increases. Both ordered and disordered regions were observed with spatially resolved measurements in a monolayer film with relatively low surface density.

Acknowledgements

The authors gratefully acknowledge DOE-PAIR (DE-FG02-99-ER45794), NSF-DMR (9812088), and NSF-SGER-CHEM (0228839) for partial support during the course of this work.

References

[1] D.L. Elmore, C.L. Leverette, A.T. Kalambur, Y. Liu, D.B. Chase, J.F. Rabolt, Langmuir 19 (2003) 3519.
[2] A. Ulman, An Introduction to Ultrathin Organic Thin Films from Langmuir Blodgett to Self-Assembly, Academic Press, San Diego, 1991.
[3] A. Ulman, Chem. Rev. 96 (1996) 1533.
[4] D.L. Angst, G.W. Simmons, Langmuir 7 (1991) 2236.
[5] I. Willner, A. Schlittner, A. Doron, E. Joselevich, Langmuir 15 (1999) 2766.
[6] D. Allara, Biosens. Bioelectron. 10 (1995) 771.
[7] T. Komeda, K. Namba, Y. Nishioka, J. Vac. Sci. Technol. 3 (1998) 1680.
[8] N.L. Jeon, K. Finnie, K. Branshaw, R.G. Nuzzo, Langmuir 13 (1997) 3382.

[9] R.A. Dluhy, S.M. Stephens, S. Widayati, A.D. Williams, Spectrochim. Acta A 51 (1995) 1413.
[10] S.R. Wasserman, Y.-T. Tao, G.M. Whitesides, Langmuir 5 (1989) 1074.
[11] J. Lobau, A. Rumpphorst, G. Gall, S. Seeger, K. Wolfrun, Thin Solid Films 289 (1996) 272.
[12] N. Mino, K. Nakajima, K. Ogawa, Langmuir 7 (1991) 1468.
[13] R.G. Greenler, J. Chem. Phys. 44 (1966) 310.
[14] J.F. Rabolt, F.C. Burns, N.E. Schlotter, J. Swalen, J. Chem. Phys. 78 (1983) 946.
[15] H. Brunner, U. Mayer, H. Hoffman, Appl. Spectrosc. 51 (1997) 209.
[16] E.N. Lewis, P.J. Treado, R.C. Reeder, G.M. Story, A.E. Dowrey, C. Marcott, I.W. Levin, Anal. Chem. 67 (1995) 3377.
[17] E.N. Lewis, A.M. Gorbach, C. Marcott, I.W. Levin, Appl. Spectrosc. 50 (1996) 263.
[18] R. Bhargava, I.W. Levin, Anal. Chem. 73 (2001) 5157.
[19] C. Marcott, R.C. Reeder, E.P. Paschalis, D.N. Tatakis, A.L. Boskey, R. Mendelsohn, Cell. Mol. Biol. 44 (1998) 109.
[20] C.M. Snively, J.L. Koenig, Macromolecules 31 (1998) 3753.
[21] R. Mendelsohn, E.P. Paschalis, A.L. Boskey, J. Biomed. Optics 4 (1999) 14.
[22] R. Bhargava, T. Ribar, J.L. Koenig, Appl. Spectrosc. 53 (1999) 1313.
[23] R. Bhargava, S.Q. Wang, J.L. Koenig, Appl. Spectrosc. 54 (2000) 486.
[24] D.L. Elmore, M.W. Tsao, S. Frisk, D.B. Chase, J.F. Rabolt, Appl. Spectrosc. 56 (2002) 145.
[25] W. Kern, D.A. Puotinen, RCA Rev. (1970) 187.
[26] R.C. Spiker, I.W. Levin, Biochim. Biophys. Acta 388 (1975) 361.
[27] R.G. Snyder, S.L. Hsu, S. Krimm, Spectrochim. Acta A 34A (1978) 395.
[28] R.G. Snyder, H.L. Strauss, C.A. Elliger, J. Phys. Chem. 86 (1982) 5145.
[29] R.G. Snyder, J. Chem. Phys. 47 (1967) 1316.
[30] L. Netzer, R. Iscovici, J. Sagiv, Thin Solid Films 100 (1983) 67.
[31] R. Maoz, J. Sagiv, J. Colloid Interface Sci. 100 (1984) 465.
[32] D. Lin-Vien, N.B. Colthup, W.G. Fately, J.G. Grasselli, The Handbook of Infrared and Raman Characteristic Frequencies of Organic Molecules, Academic Press, London, 1991.
[33] M.J. Lercel, R.C. Tiberio, P.F. Chapman, H.G. Craighhead, C.W. Sheen, A.N. Parikh, D.L. Allara, J. Vac. Sci. Technol. B 11 (1993) 2823.